

Self-adaptive torsional and bending flaps for drag reduction in the squareback Ahmed body wake

J. M. Camacho-Sánchez, M. Lorite-Díez, J. I. Jiménez-González, C. Martínez-Bazán and O. Cadot.

ERCOFTAC SPRING FESTIVAL 2024

15-17 April 2024, UC3M, Spain



UNIVERSIDAD
DE GRANADA

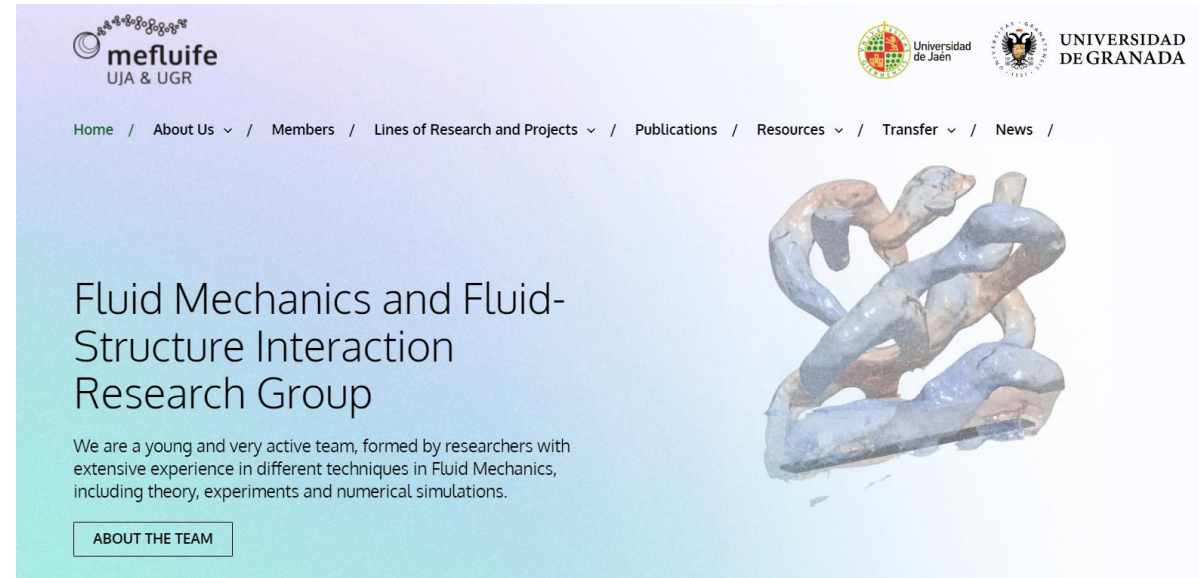
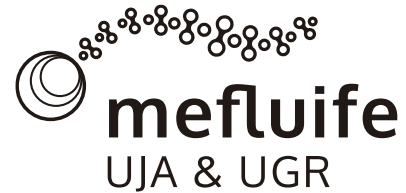
UJa Universidad
de Jaén



UNIVERSITY OF
LIVERPOOL

MEFLUIFE GROUP

- 6 permanent members
- 2 postdocs
- 4 PhD students
- 2 technicians

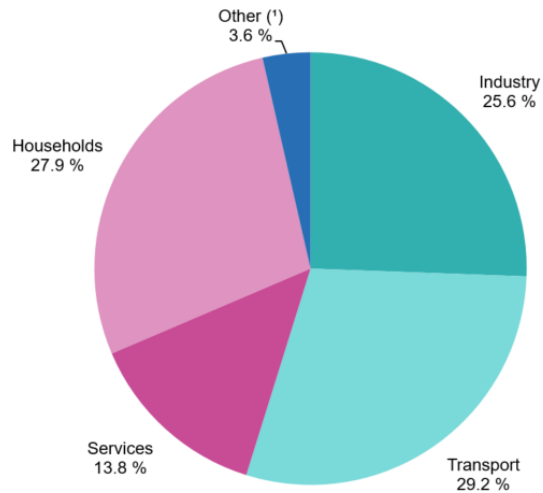


- Main research lines:
 - Multiphase flows: bubble dynamics
 - Bluff body wakes & FSI
 - Biomedical flows: CSF Flow

Motivation

- Energy consumption in transport industry

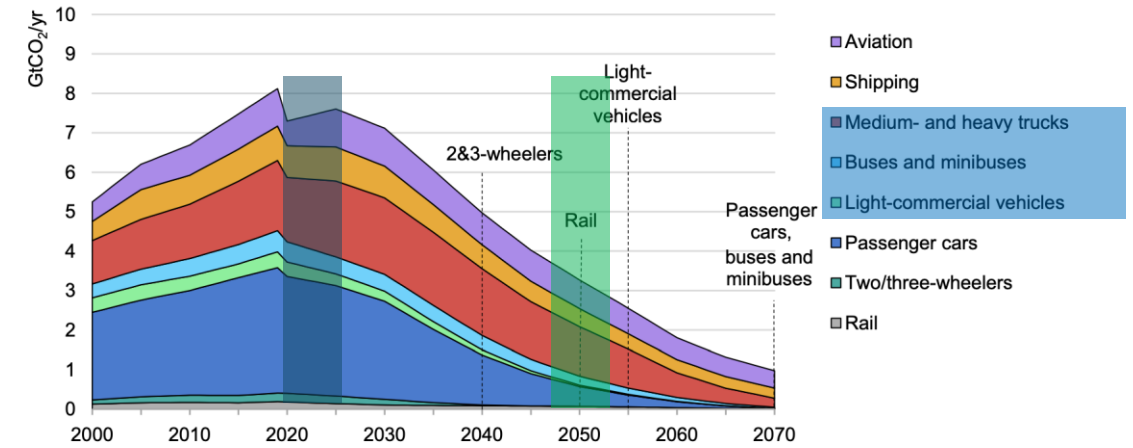
Final energy consumption by sector, EU, 2021
(% of total, based on terajoules)



(*) International aviation and maritime bunkers are excluded from category Transport.
Source: Eurostat (online data code: nrg_bal_c)



Figure 3.16 Global CO₂ emissions in transport by mode in the Sustainable Development Scenario, 2000-70



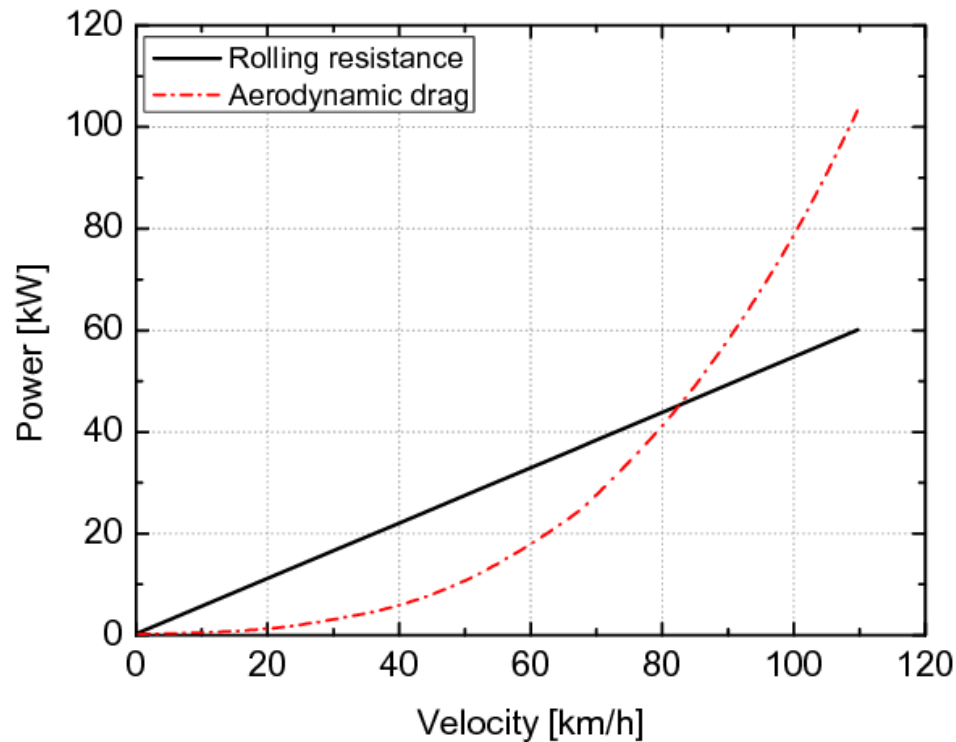
IEA 2020. All rights reserved.



Introduction

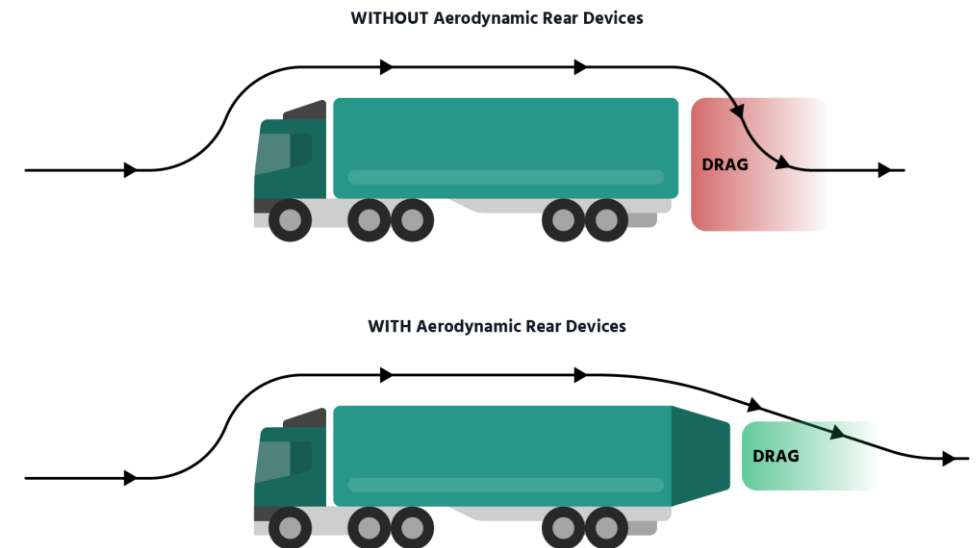
- Reduce aerodynamic drag in heavy vehicles (lower emissions)
- Load capacity, practical requirements
- New regulations, great potential technological impact

Directive Europe 96/53/EC modified in EU 2015/719 and updated with the new legislation 2018/0130



ICCT (International Council on Clean Transportation)

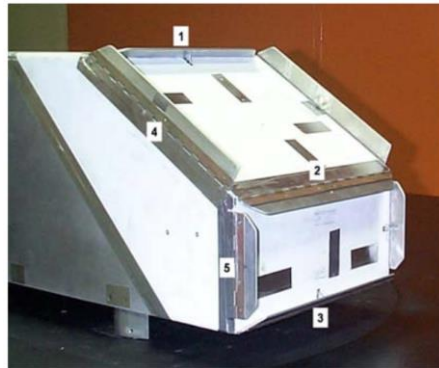
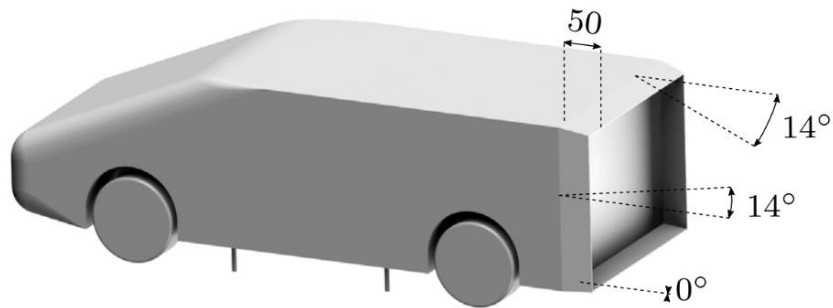
PRESSURE DRAG ON TRUCKS



Introduction

- Vehicle models, drag reduction devices and physical mechanisms

Urquhart et al. (IJHFF 2020)



Beaudoin & Aider (EiF 2008)

Barros et al. (JFM 2016)

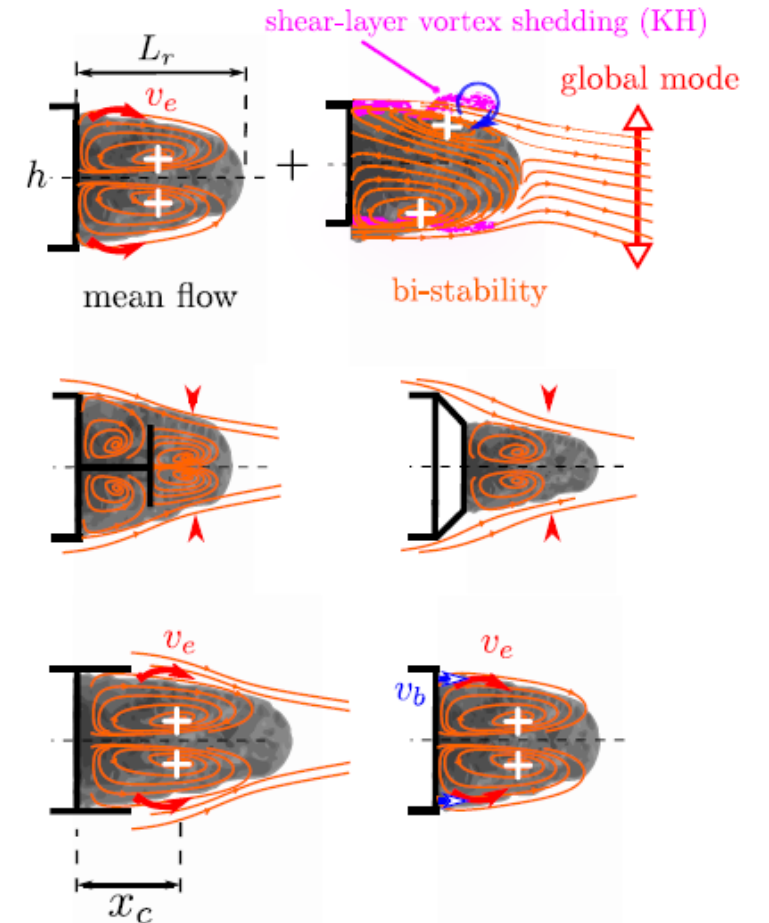
Reduced entrainment

Bubble elongation

Aerodynamic wake shaping

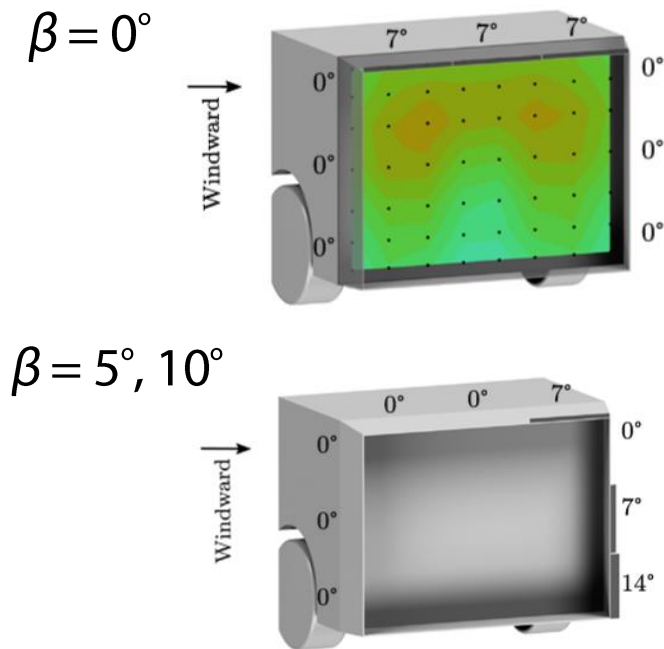
Reduced wake bluntness

Plumujeau et al. (EJMB 2023)

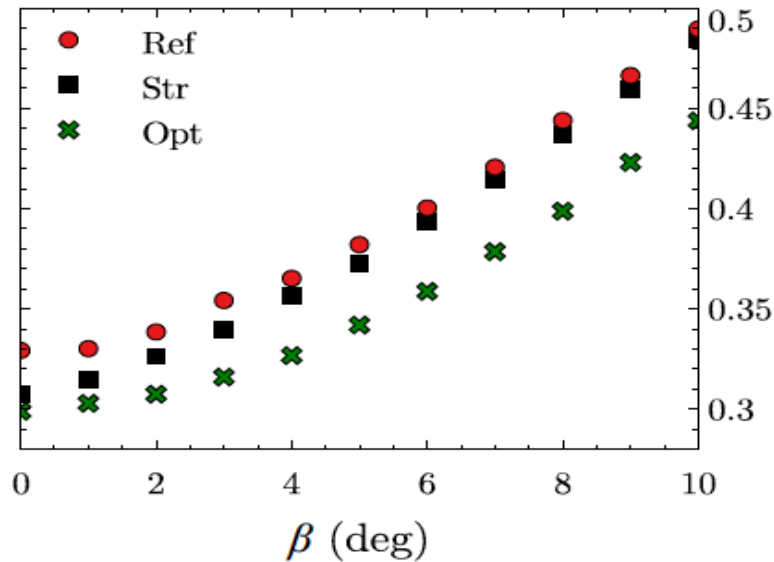


Introduction

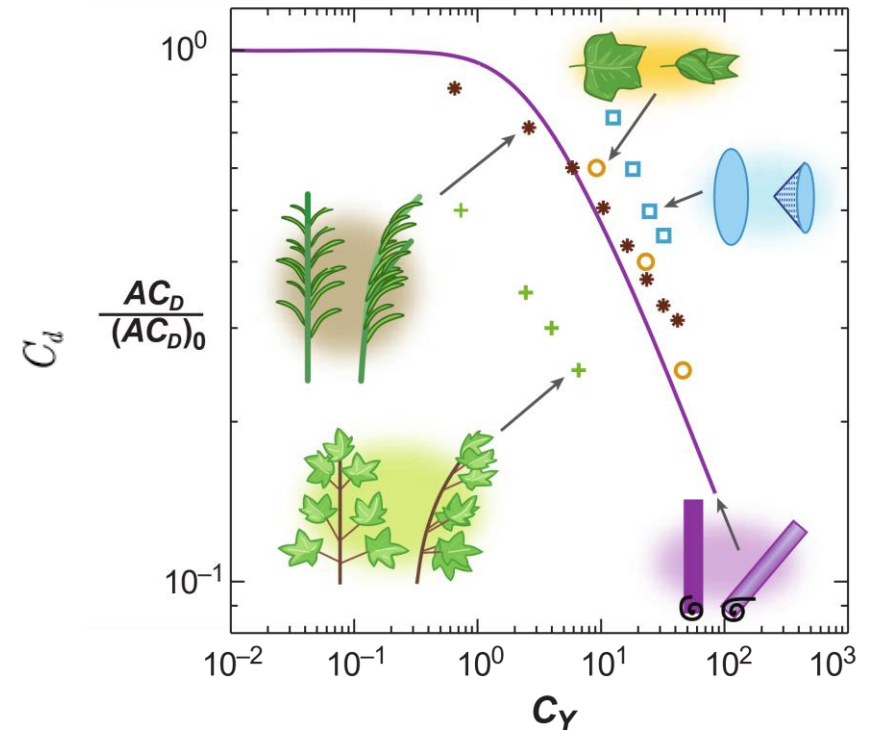
- Rigid passive devices
 - Limited efficiency in changing flow conditions
 - Crosswinds, different turbulent levels and gusts are common in real applications
 - Can we use bio-inspired self-adaptive devices?



Urquhart et al. (IJHFF 2020)



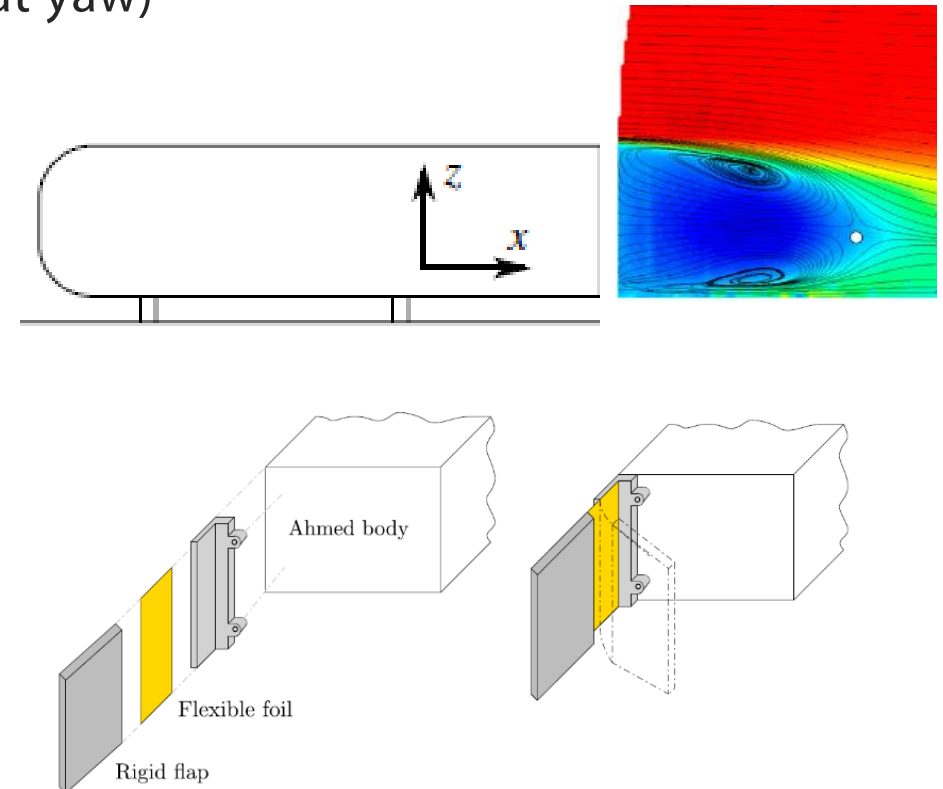
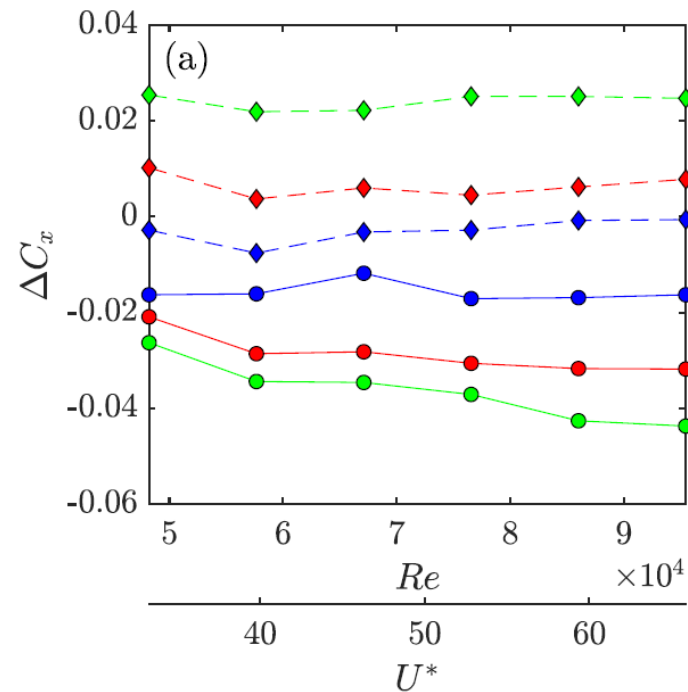
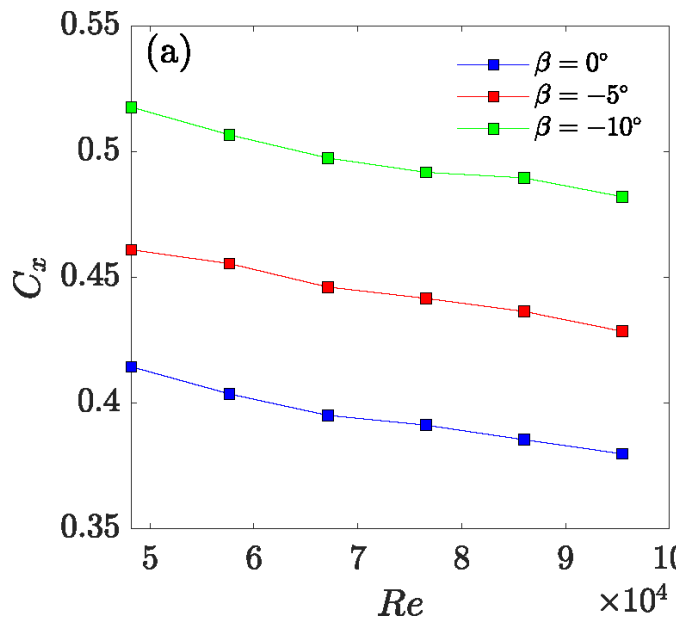
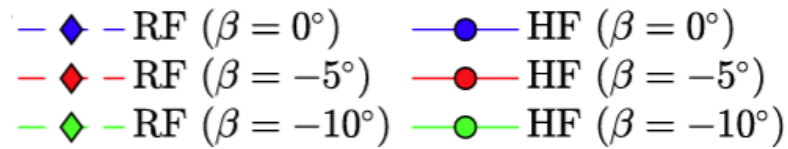
Lorite-Díez et al. (JWEIA 2020)



De Langre (ARFM 2008)

Previous Results

- 1 Degree-of-freedom hinged flaps
 - Rotary flaps are efficient to reduce the drag (especially at yaw)



Camacho-Sánchez et al. (PRF 2023)

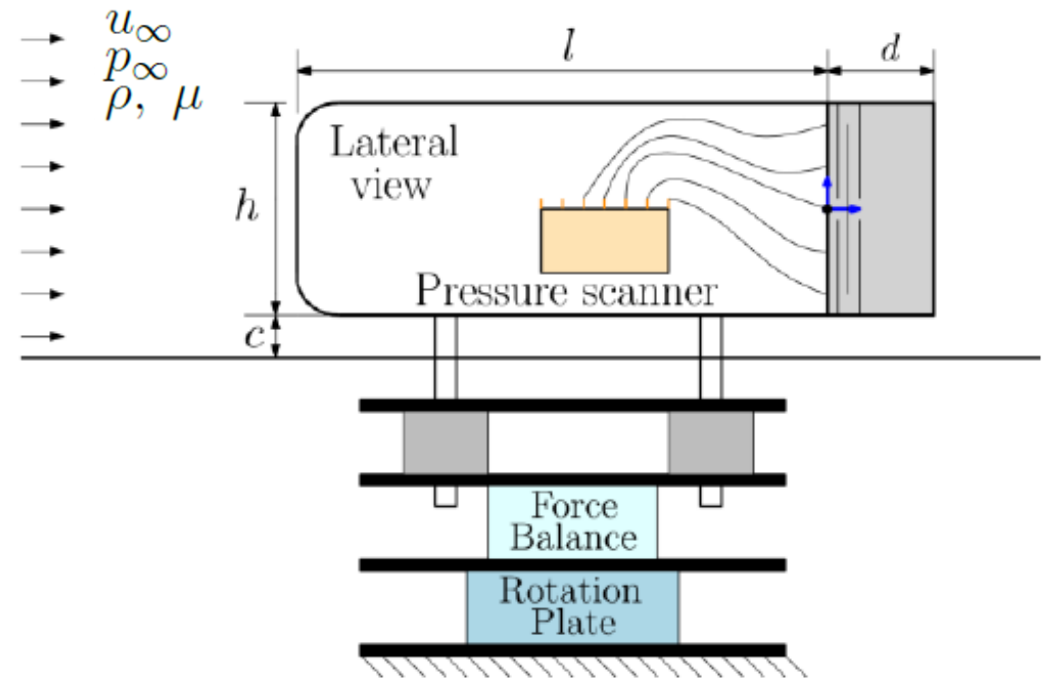
Experimental set-up

- Parametric ranges
 - Reynolds from $1.5e5$ to $2.3e5$
 - Flaps length (d) around $0.5h$
 - Large mass ratios ~ 320
 - Reduced velocity U^* from 14 to 22
 - Different yaw orientations, β (-15:1:15)

$$Re = \frac{\rho u_{\infty} h}{\mu}$$

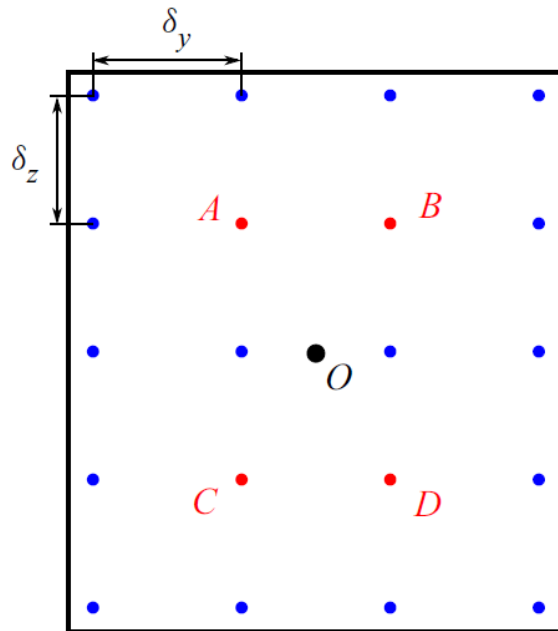
$$m^* = \rho_s / \rho$$

$$U^* = \frac{u_{\infty}}{f_n h}$$



Experimental set-up

- Measurements
 - 6 axis force balance
 - 64 channel miniature pressure scanner
 - Laser point distance sensors
 - High-speed imaging
 - StereoPIV measurements



Pressure

$$c_{p,i} = \frac{p_i - p_\infty}{\rho u_\infty^2 / 2}$$

$$c_B = -\frac{1}{n} \sum_{i=1}^n c_{p,i}$$

$$g_y = h \frac{\partial c_p}{\partial y} \simeq \frac{1}{2} h \left[\frac{c_{p,6} - c_{p,4}}{y_6 - y_4} \right]$$

$$g_z = h \frac{\partial c_p}{\partial z} \simeq \frac{1}{2} h \left[\frac{c_{p,8} - c_{p,2}}{z_8 - z_2} \right]$$

Forces

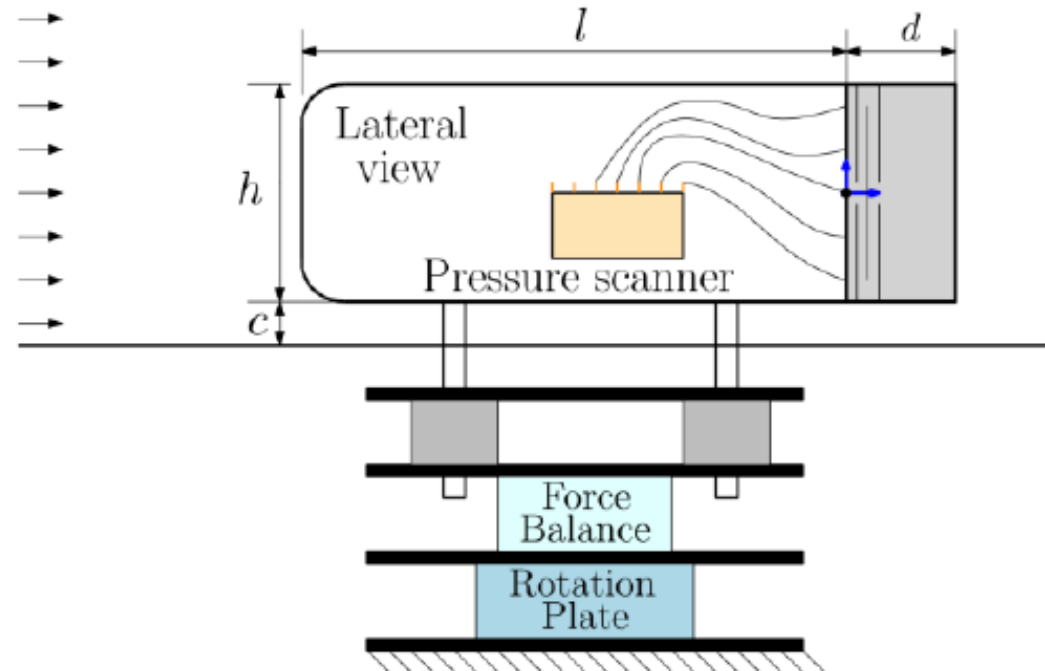
$$C_i = \frac{2f_i}{\rho u_\infty^2 h w}$$

Nomenclature

$$A = \bar{a}$$

$$a' = a - A$$

$$\hat{a} = \sqrt{a'^2}$$

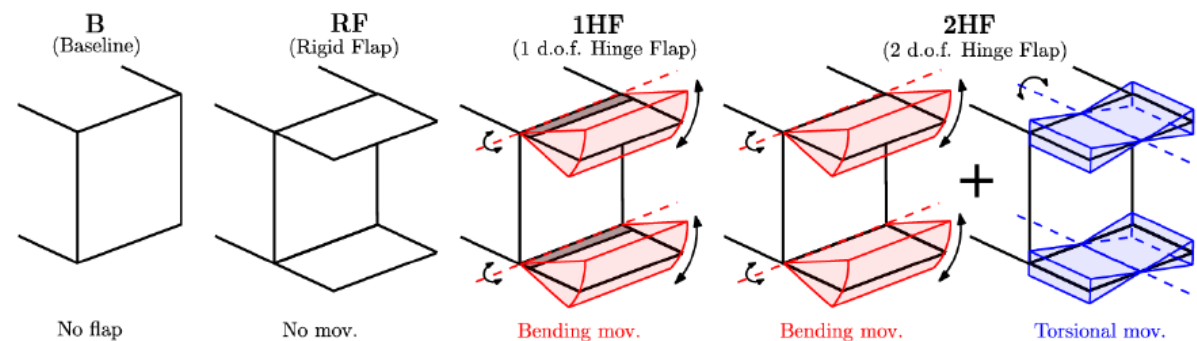
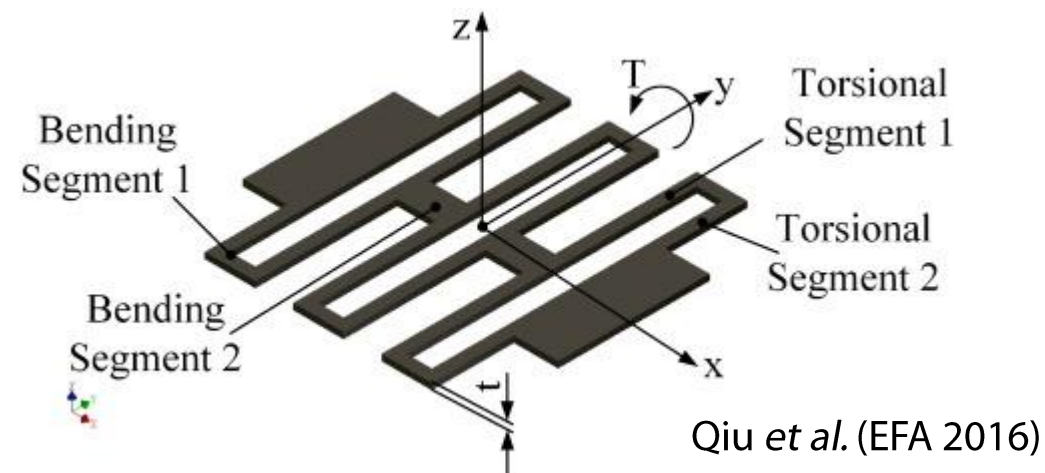


Results

- 2 Degree-of-freedom hinged flaps
 - Several configurations (RF, 1H, 2H)
 - Left-Right (LR), Top-Bottom (TB) dispositions

#	TOP	BOTTOM	LEFT/RIGHT
1	-	-	-
2	RF	RF	-
3	-	-	RF
4	RF	RF	RF
5	1H	1H	-
6	-	-	1H
7	2H	2H	-
8	-	-	2H

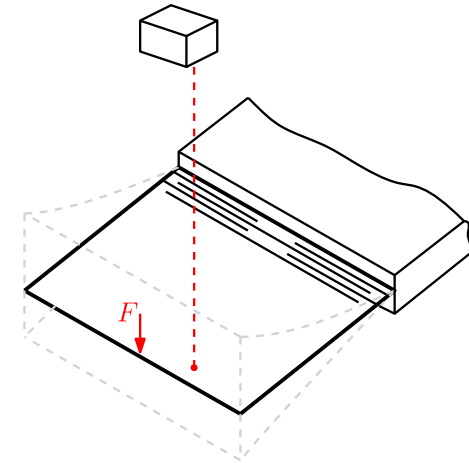
- **B** = Baseline case
- **RF** = Rigid flap
- **1H** = 1 DoF Hinge flap
- **2H** = 2 DoF Hinge flap



Results

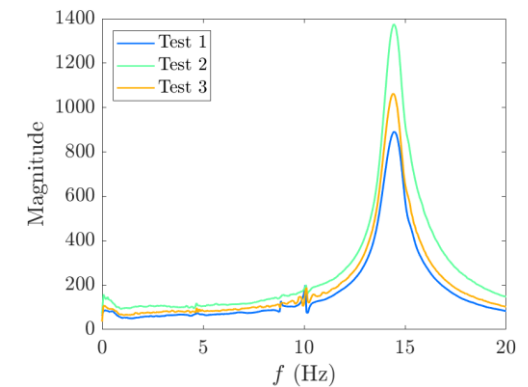
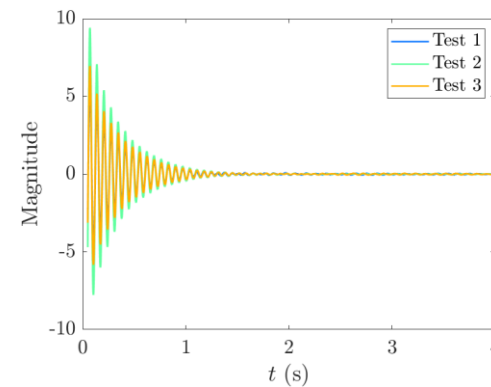
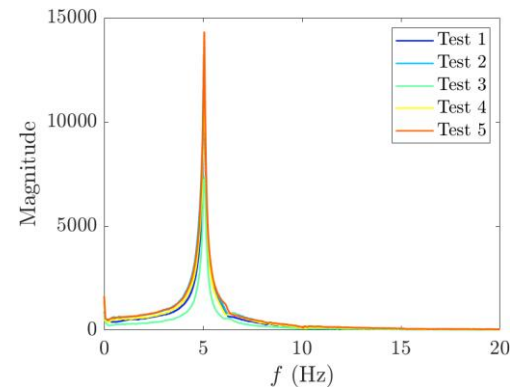
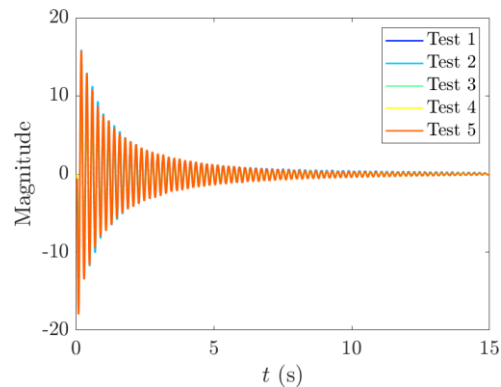
- 2 Degree-of-freedom hinged flaps
 - Several configurations
 - Mechanical characterization

Var.	1H	1H	2H	2H
$f_{n,b}$ (Hz)	3.8	3.7	3.9	3.8
$f_{n,t}$ (Hz)	-	-	16.8	16.8
ξ_b	0.026	0.025	0.019	0.019
ξ_t	-	-	0.0100	0.009
m^*	320	320	320	320



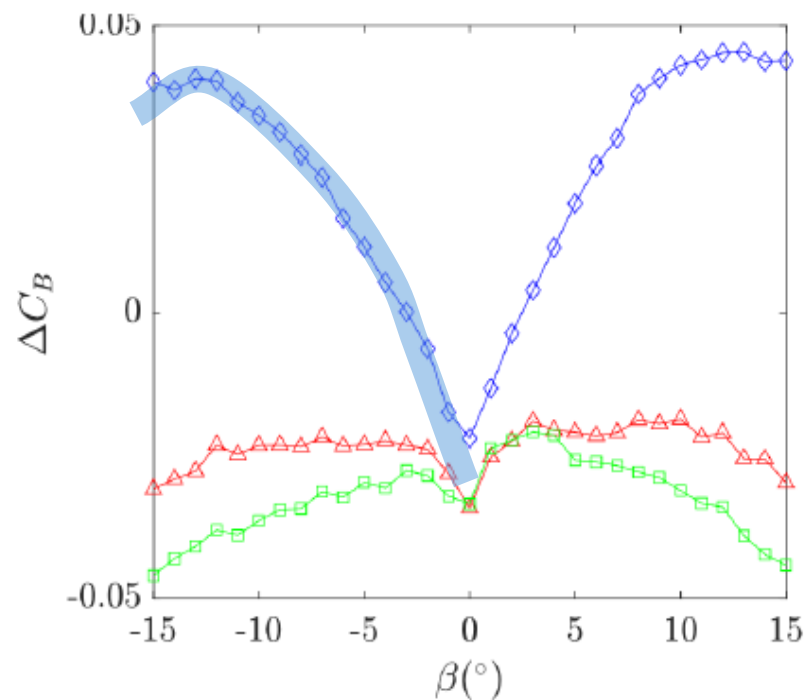
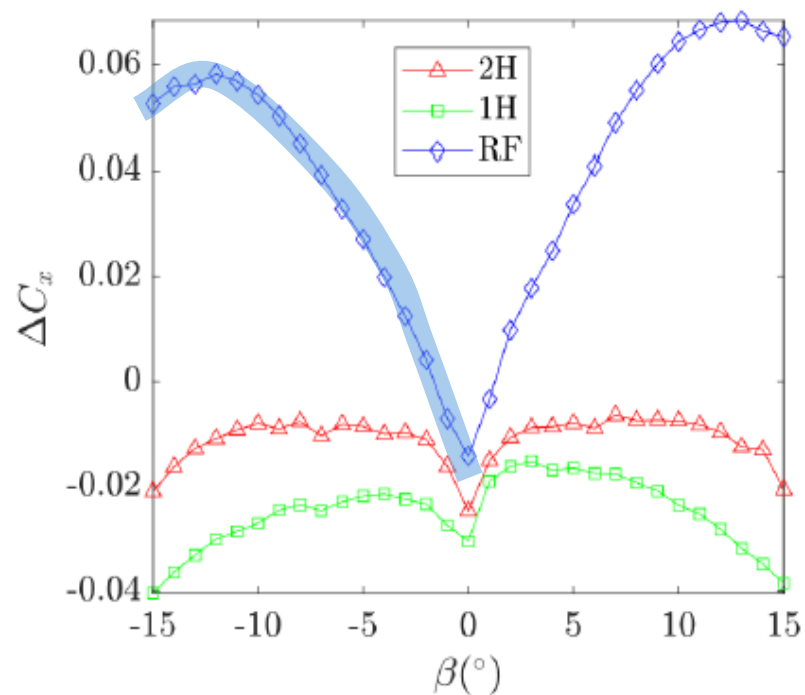
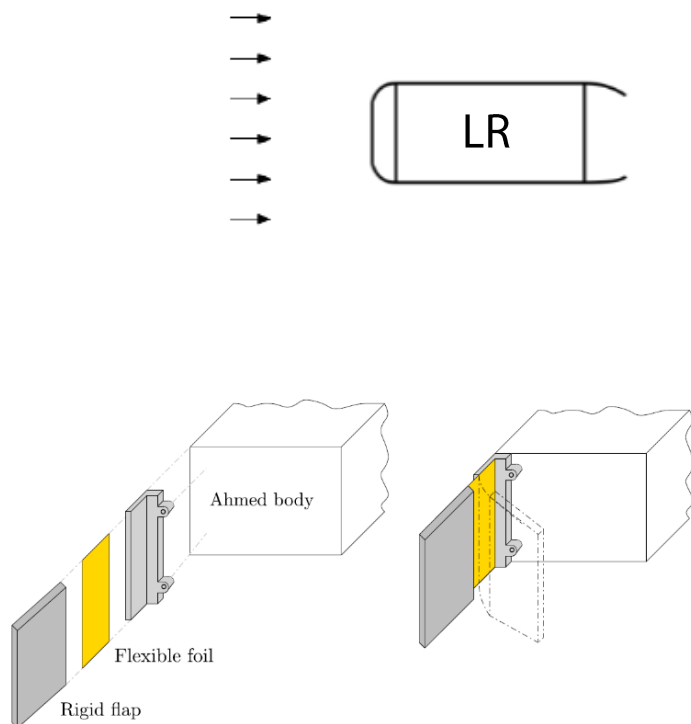
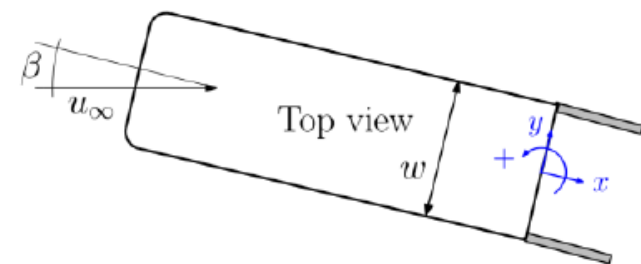
Bending

Torsional



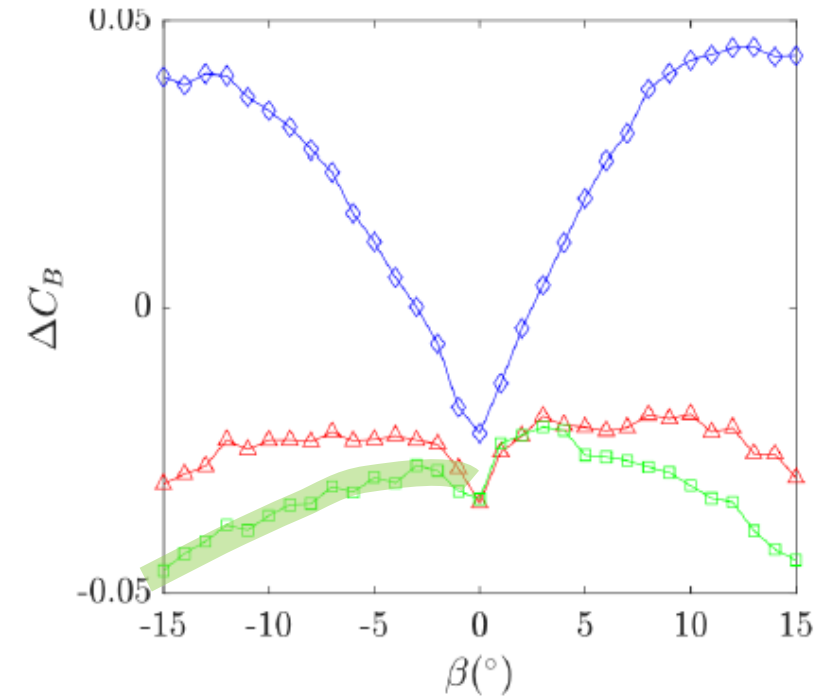
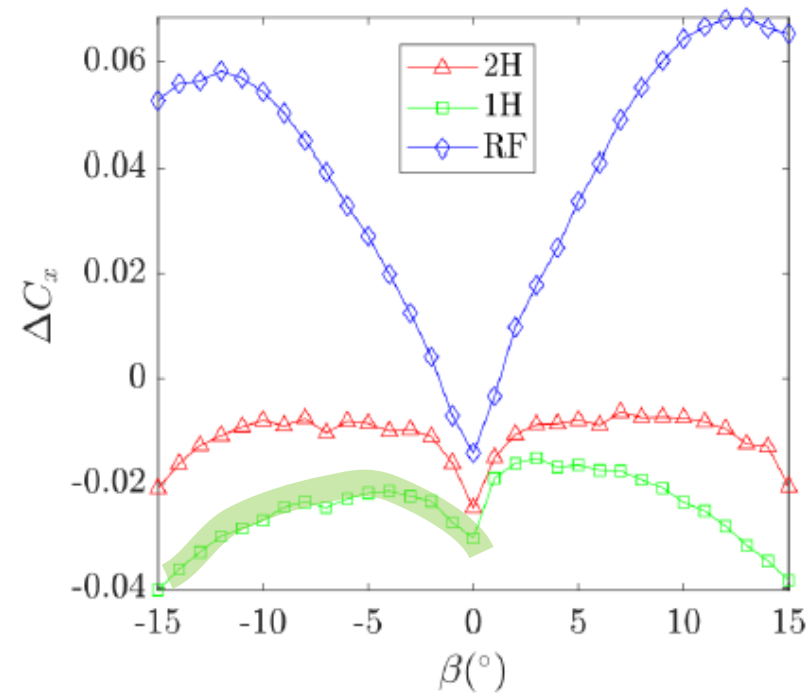
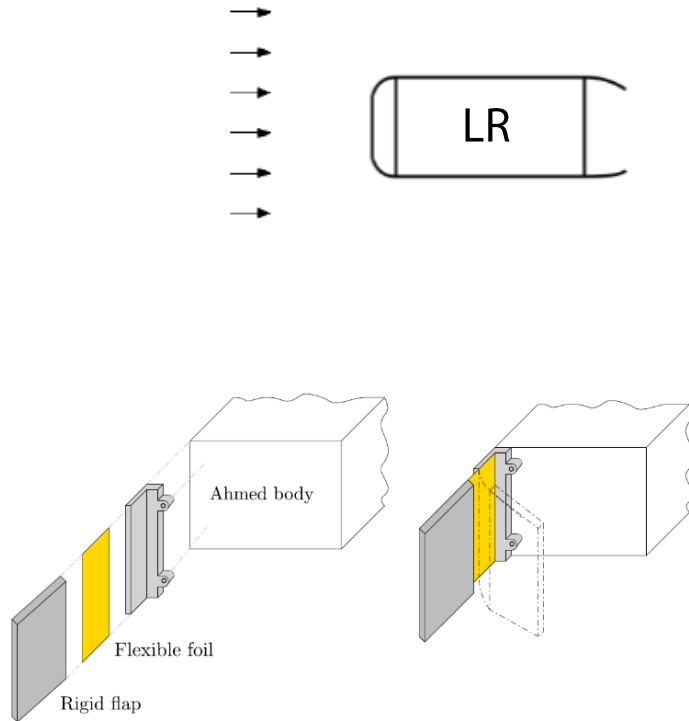
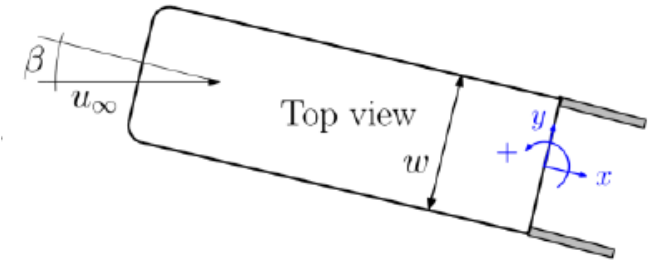
Results

- 2 Degree-of-freedom hinged flaps
 - $U^* = 18.4$ (bending), $Re = 1.87 \cdot 10^5$
 - Under LR configuration, RF only works at $\beta = 0^\circ$



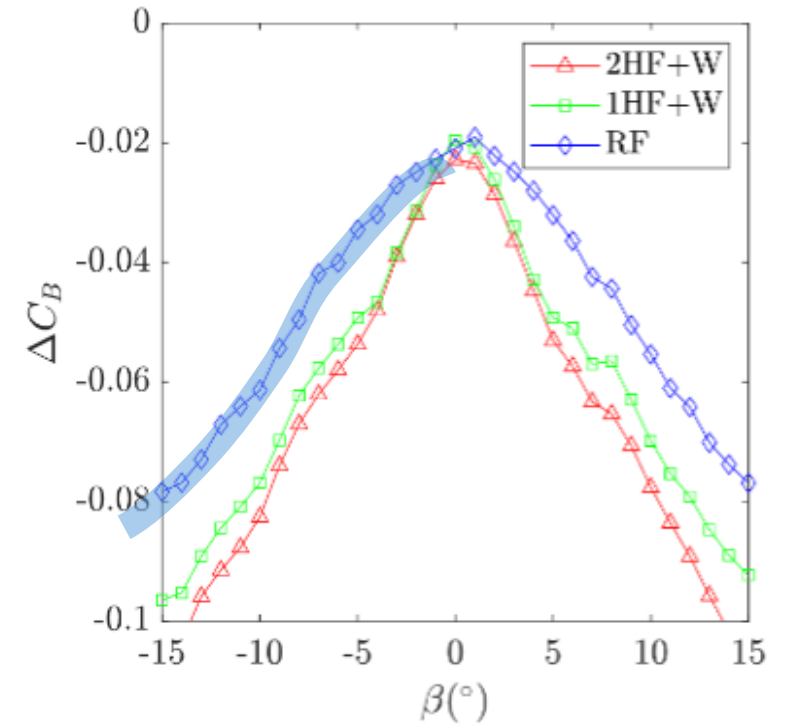
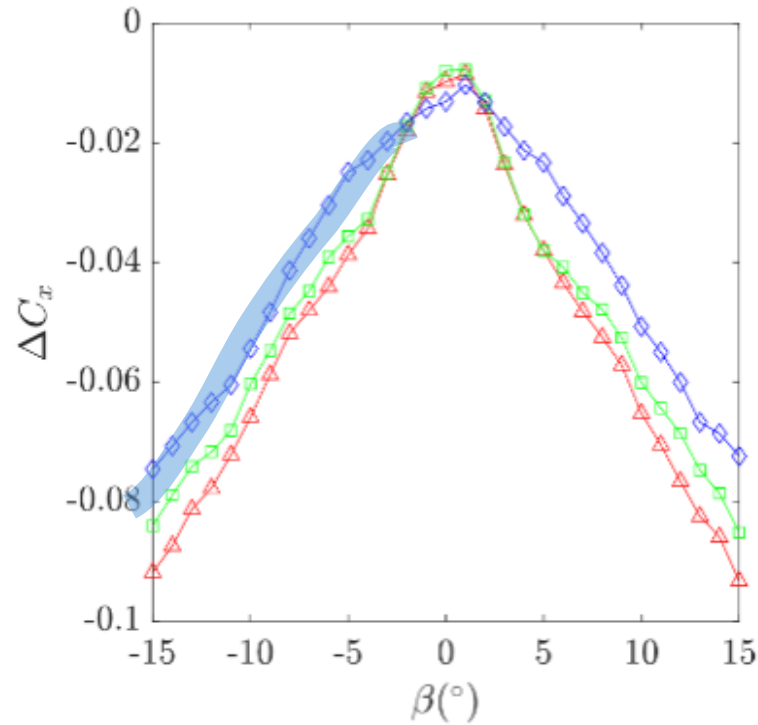
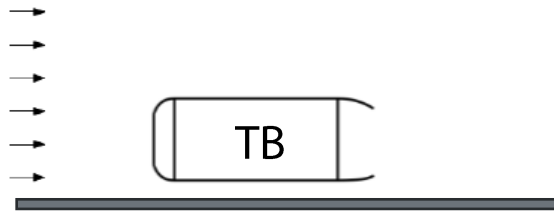
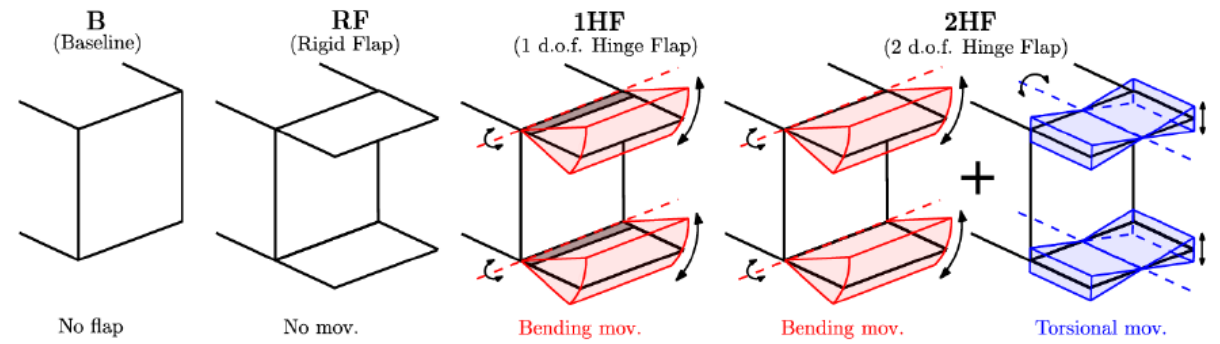
Results

- 2 Degree-of-freedom hinged flaps
 - $U^* = 18.4$ (bending), $Re = 1.87 \cdot 10^5$
 - Under LR configuration, 1HF is the best option



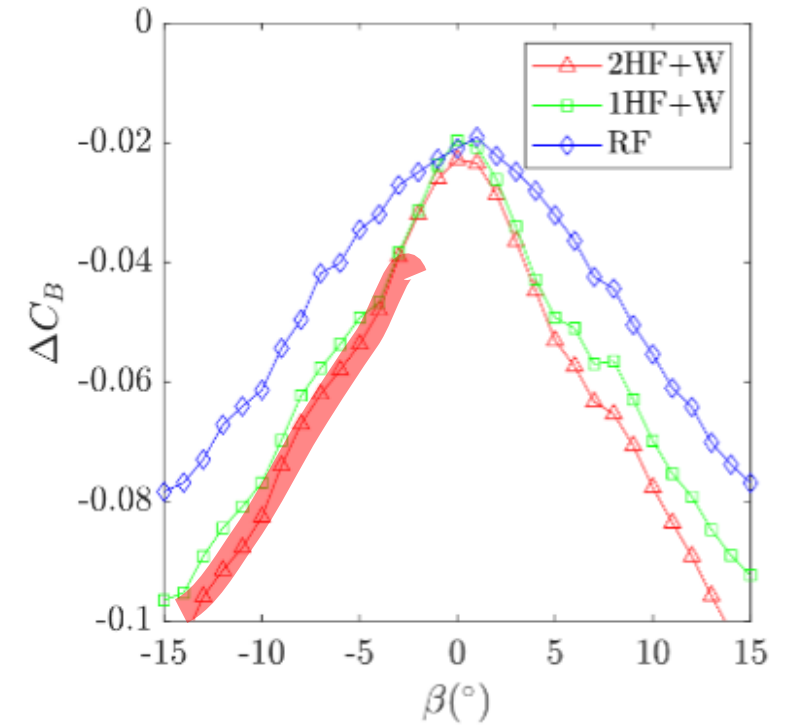
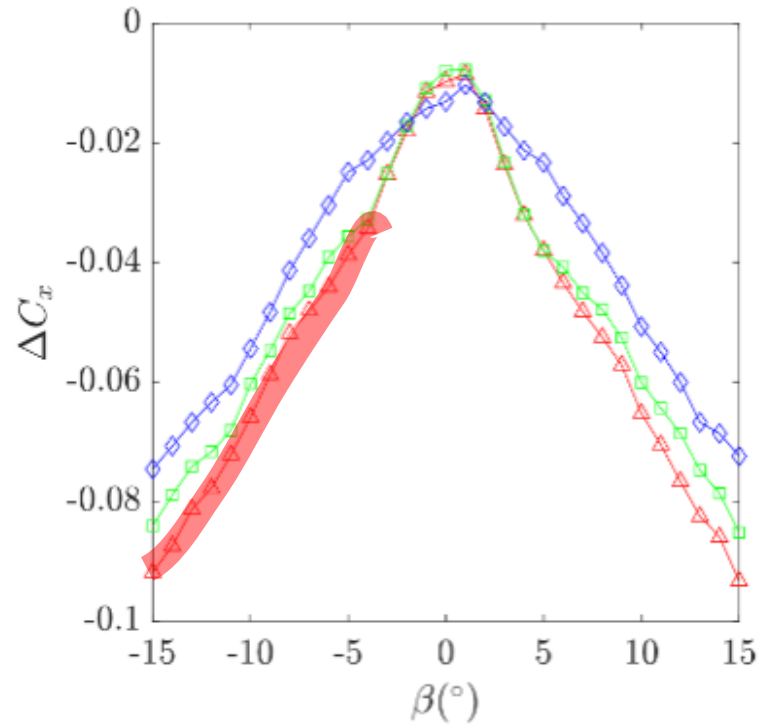
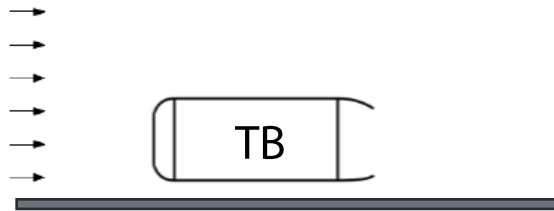
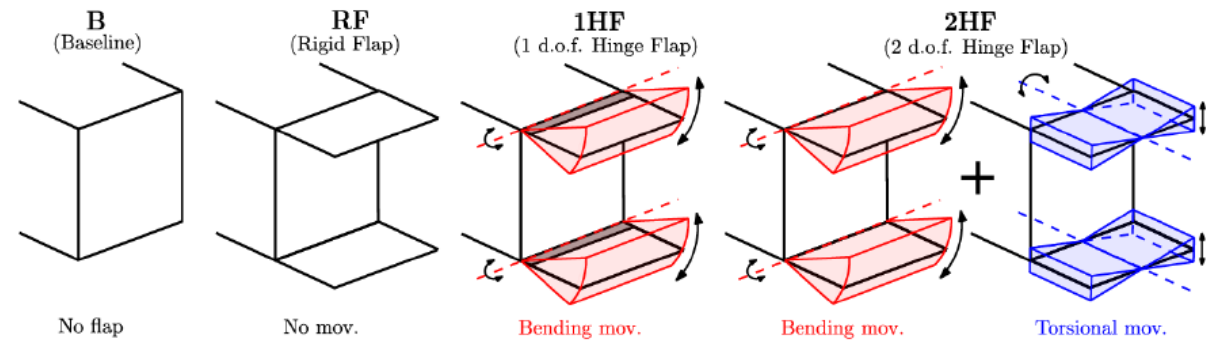
Results

- 2 Degree-of-freedom hinged flaps
 - $U^* = 18.4$ (bending), $Re = 1.87 \cdot 10^5$
 - Under TB configuration, RF is effective



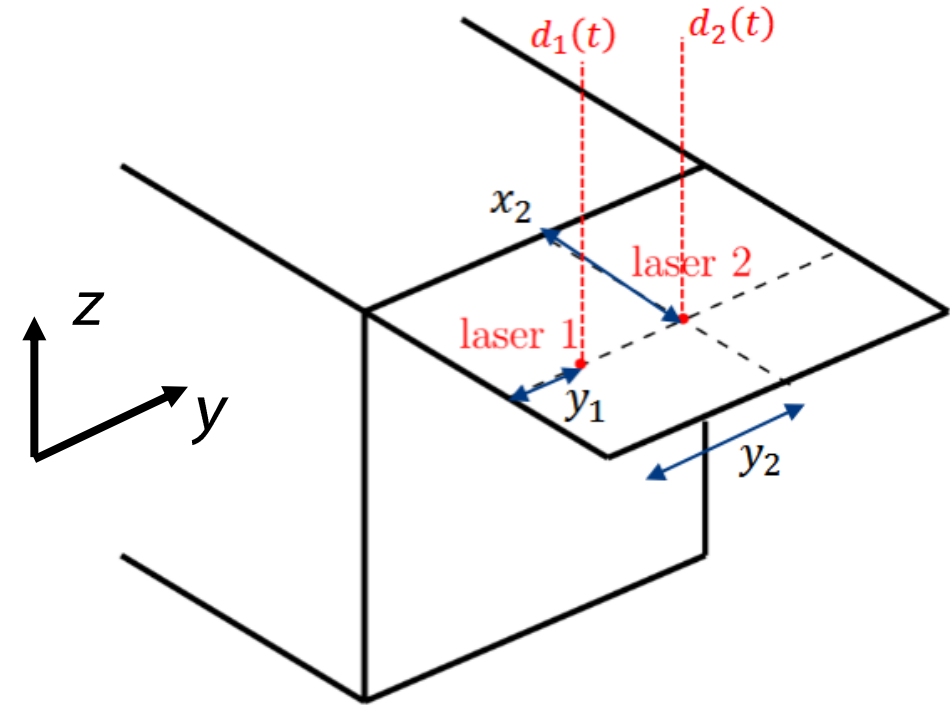
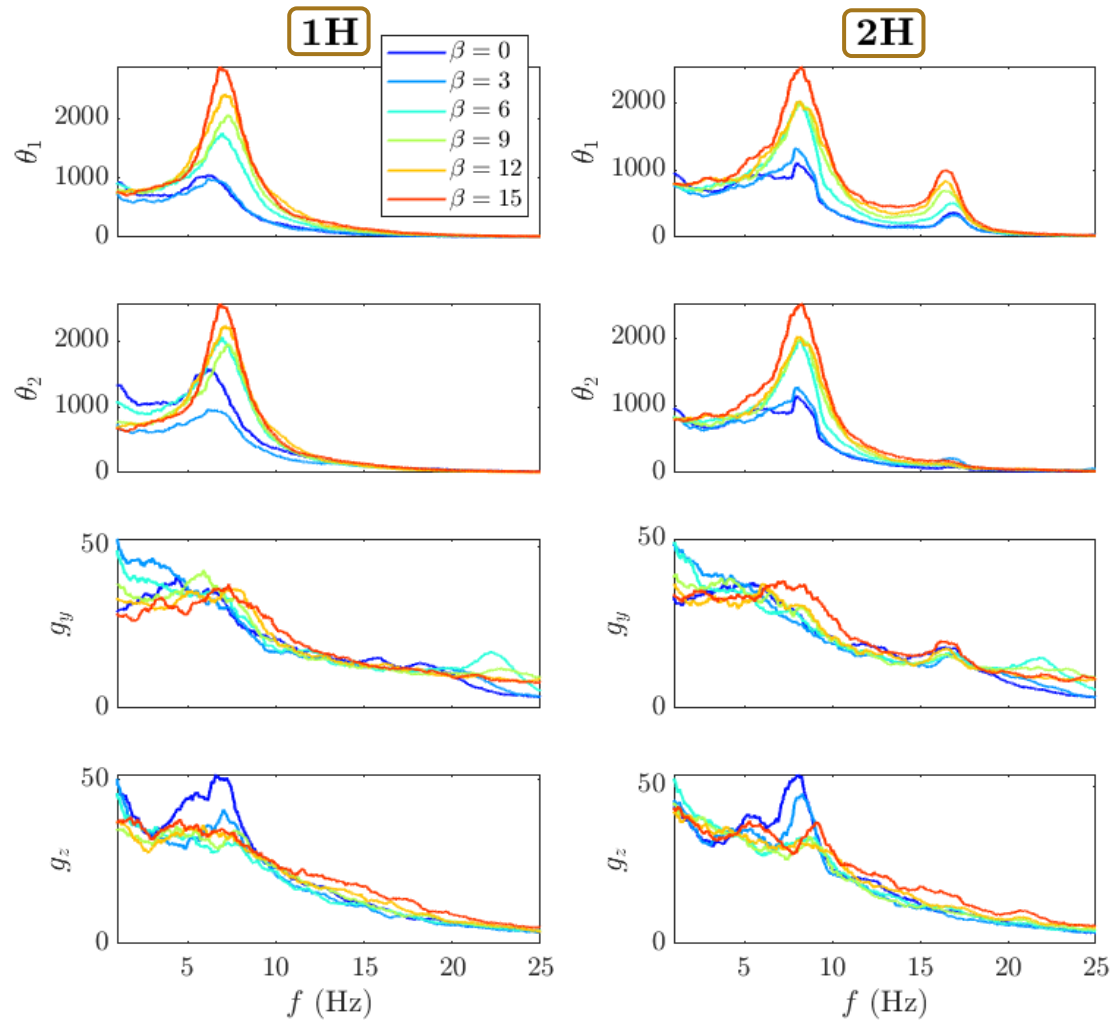
Results

- 2 Degree-of-freedom hinged flaps
 - $U^* = 18.4$ (bending), $Re = 1.87 \cdot 10^5$
 - Under TB, 2HF improves with yaw



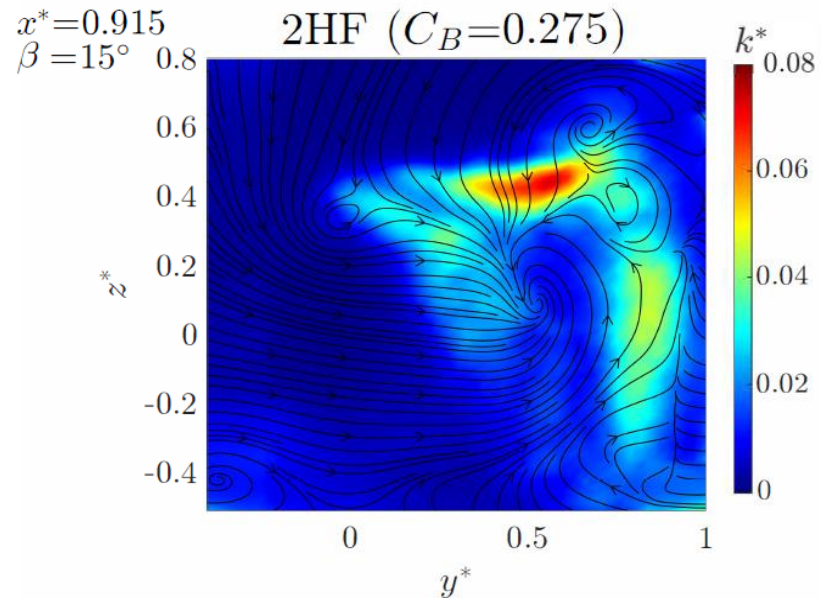
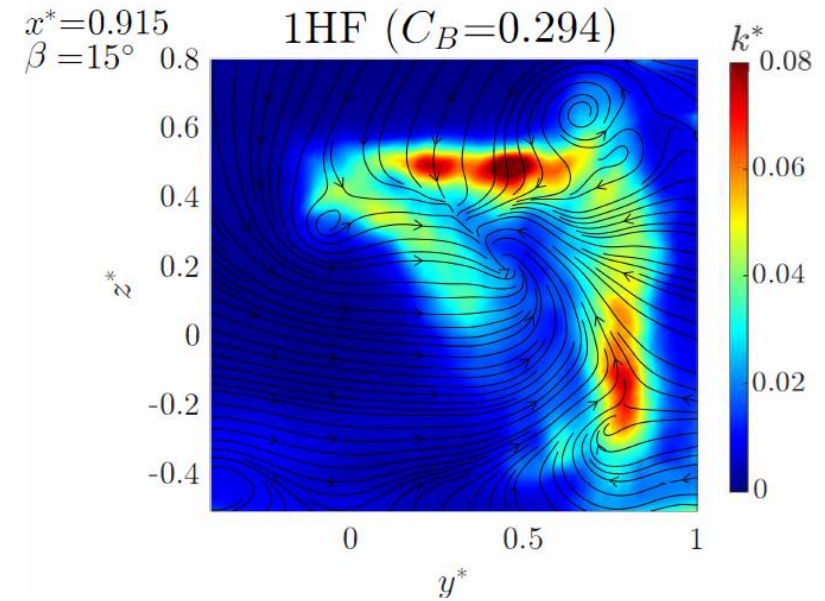
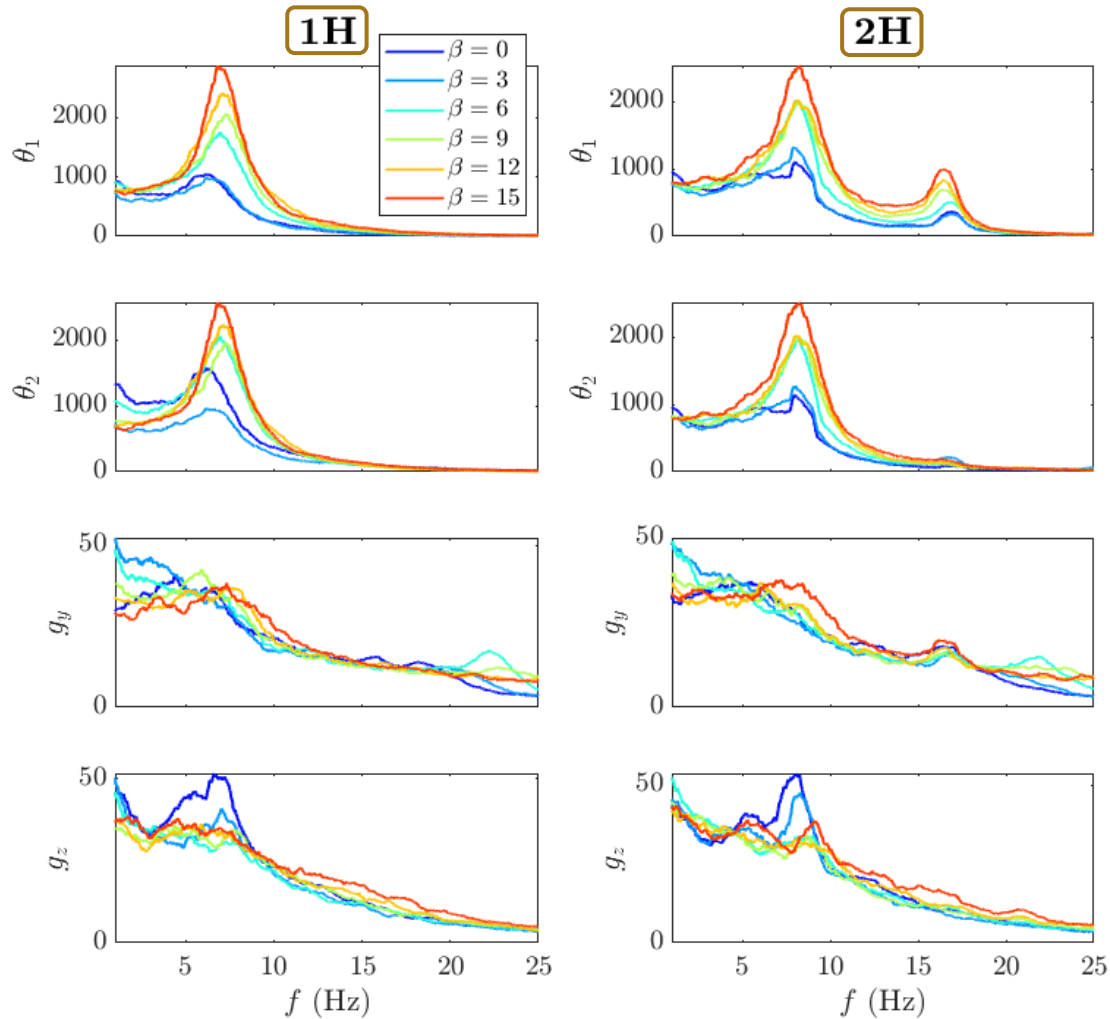
Results

- 2 Degree-of-freedom hinged flaps
 - 2HF starts to modify the wake at $\beta > |5^\circ|$



Results

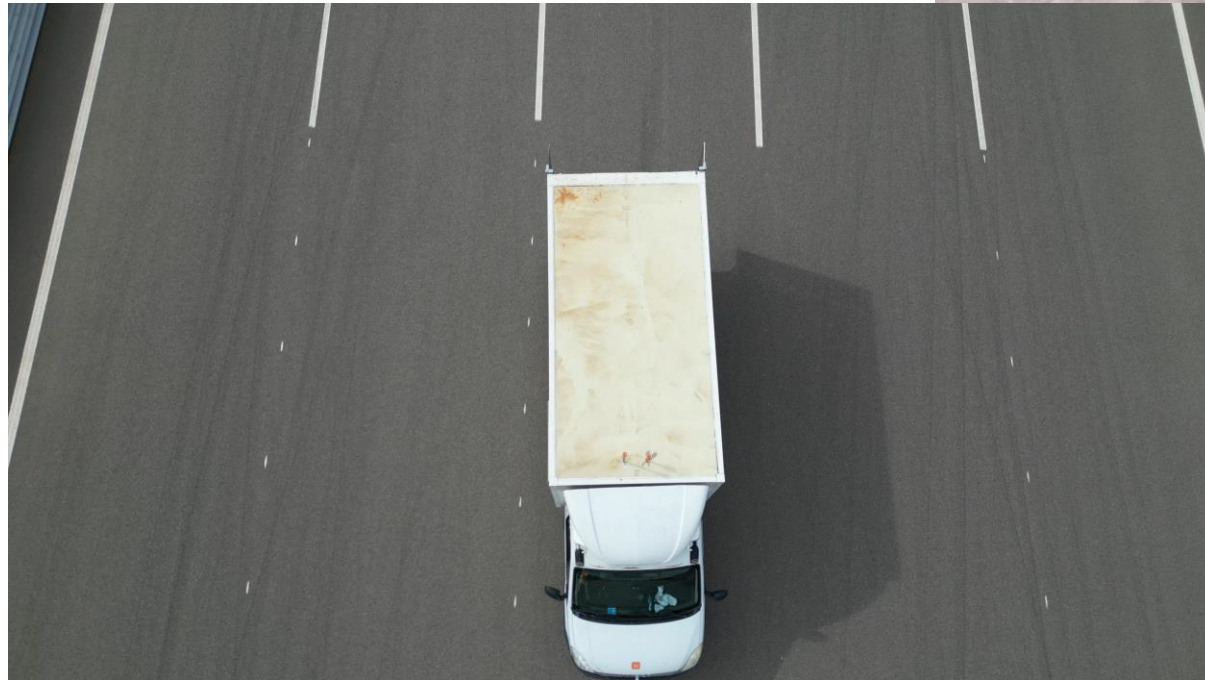
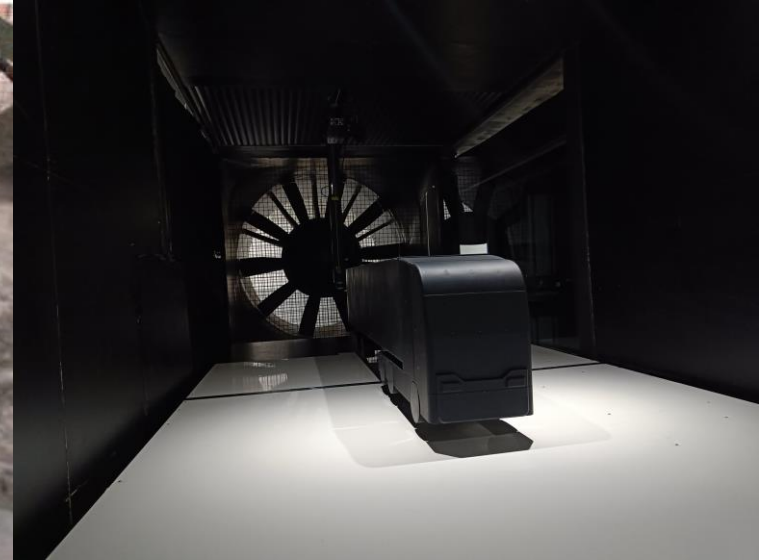
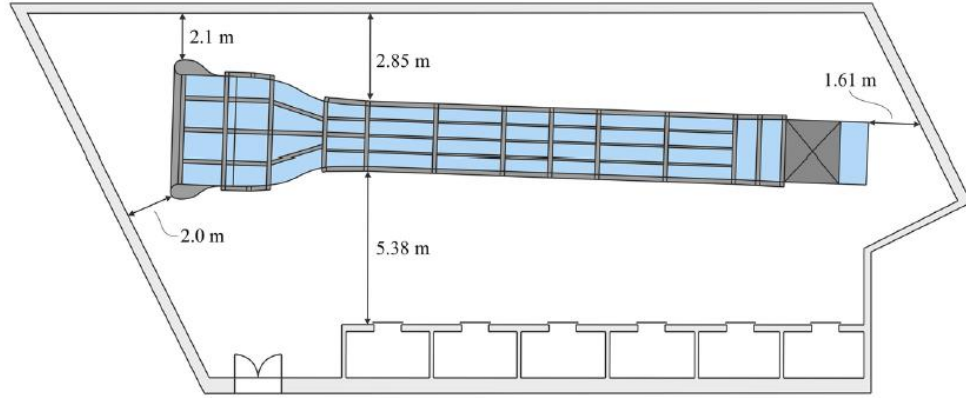
- 2 Degree-of-freedom hinged flaps
 - 2HF starts to modify the wake at $\beta > |5^\circ|$



Conclusions

- 3D Self-adaptive flaps with different DoF are able to reduce C_D under different flow conditions
- For reducing drag under yaw, TB configurations are better than LR
- The increase of degrees of freedom improves the performance under yaw
- The DoF of the flaps show different FSI mechanisms with the 3D wake
- Flexible flaps could help in the design of real and effective drag reduction devices

Ongoing works



Thank you for your attention

Questions?

The authors gratefully **acknowledge** the funding provided by the projects TED2021-131805B-C21, TED2021-131805B-C22 and PID2022-140433NA-I00 financed by the Spanish MCIN/AEI/10.13039/501100011033/, the European Union NextGenerationEU/PRTR and FEDER, UE respectively.

